X-750-73-244

# STUDY OF EQUATORIAL SCINTILLATIONS
# A PROGRESS REPORT

DECEMBER 1972

GODDARD SPACE FLIGHT CENTER
GREENBELT, MARYLAND

X-750-73-244

# STUDY OF EQUATORIAL SCINTILLATIONS

## A PROGRESS REPORT

José Pomalaza
Ronald Woodman
Gilberto Tisnado
Eduardo Nakasone

Instituto Geofisico del Peru

December 1972

GODDARD SPACE FLIGHT CENTER
Greenbelt, Maryland

CONTENTS

## ILLUSTRATIONS

# STUDY OF EQUATORIAL SCINTILLATIONS

## INTRODUCTION

Observations of amplitude scintillations produced by F-Region ionospheric irregularities has been performed at the Ancón Observatory (Latitude -11°46', Longitude 77°9') since 1968. At first Minitrack interferometric records at 137 MHz were used in the studies[1].

In 1969 two 136 MHz nine yagi arrays were placed 366 m. apart in an East-West (E-W) baseline to receive geostationary satellite transmissions in the presence of ionospheric irregularities; this arrangement allows a measurement of correlation distances, fading rates and E-W drifts[2]. For these observations 136 MHz transmissions of ATS-1, ATS-3 and ATS-5 satellites were used.

At the end of 1971 a 1550 MHz receiving system was installed and amplitude scintillation observation at this frequency began. For this, the L-Band transponder of the ATS-5 geostationary satellite was used.

The data collected is recorded on tape for further analysis at the Goddard Space Flight Center and at the Observatory at Jicamarca.

The purpose of this report is to present results of some of the work performed on the data during the period late 1971 and 1972.

[1]Superscripts refer to references.

# CORRELATION BETWEEN SATELLITES AND INCOHERENT RADAR OBSERVATIONS OF SCINTILLATIONS

## 1. INTRODUCTION

In an effort to obtain a more complete picture of the scintillation phenomenon concurrent observations are being performed in both Ancón and Jicamarca Observatories.

In Ancón, satellites are used to obtain the integrated effect of ionospheric irregularities and in Jicamarca the incoherent radar allows the observation of the density fluctuations, $\Delta N$, at all heights in the ionosphere.

The correlation was found to be more complicated than was expected. There are times for which the correlation is perfect and there are others in which there does not seem to be any correlation at all. In this report a hypothesis to explain these discrepancies is presented.

## 2. EQUIPMENT USED

In Ancón, a system of two spaced antennas is used to obtain information about the intensity of scintillations, fading rates, scale sizes and E-W drifts of the ionospheric irregularities[2]. Figure 1 shows a block diagram of the system and Figure 2 a sample of a pair of typical signals obtained from ATS-3.

At Jicamarca, the incoherent radar allows a determination of the relative intensity of the ionospheric density fluctuations at all heights in the ionosphere. For the purpose of this determination a film recording technique was developed. Figure 3 shows a block diagram of the device. The clock initiates a measurement of the echo power returned by the irregularities every 30 seconds. The function generator produces an exponential current to drive the current controlled attenuator producing a variable attenuation that can be directly calibrated in decibels. The output of the attenuator intensity modulates an oscilloscope and the resultant display is photographed by the camera. Figure 4 shows a typical recording of this system. Height marks occur every 100 km in the vertical axis. Every 30 seconds there is a sample of the relative power profile. The maximum attenuation is 40 db and is equal to the distance between samples in Figure 4. The first trace from the bottom is the ground echo, the second is the sporadic E layer and the others are scintillating layers.

From pictures like the one shown in Figure 4 important parameters of the irregularities can be measured such as relative intensity and the height and thickness of the layers of irregularities.

Backscatter from irregularities is aspect sensitive and practically all of the echo power comes from a direction perpendicular to the elongated irregularities. For this reason, and for the purpose of this experiment, the Jicamarca antenna is pointed toward the North so as to be perpendicular to the earth's magnetic field lines at this latitude.

For this experiment the Jicamarca antenna array was split in two and aimed in two distinct directions so as to observe a magnetic E-W baseline. This was done in an attempt to measure the drift velocity of the irregularities by correlating the echoes received by one half of the array with the echoes received by the other. This part of the experiment will not be analyzed here.

## 3. SIMULTANEOUS OBSERVATIONS ANCÓN-JICAMARCA

During 1971 and 1972 a number of simultaneous observations were performed at Ancón and Jicamarca. From these a few were optimum in the sense that the ATS-3 satellite was in a favorable position for a comparative study. It was found, in the course of this experiment that unless the ionospheric region around the ray path between ATS-3 and Ancón and the region sensed by the Jicamarca radar are sufficiently close (less than 3° apart) there is no direct correlation between the observations performed at Ancón and those performed at Jicamarca. In this report the observations performed during September 13, 1971 are analyzed.

The geometry that existed during the observations is illustrated in Figure 5. The intersection between the ATS-3 Ancón ray path and the Jicamarca beams with a plane at 400 km altitude are shown.

These intersections are projected on the horizontal plane and are called the subionospheric point of Ancón and the subionospheric point of the Jicamarca antennas. For reference, the zenith of Ancón and the intersection of the normal to the Jicamarca antenna are also shown. In this figure we can see that the East antenna of Jicamarca observes an ionospheric region which is about 20 km to the magnetic west of the region observed by Ancón. The signals received by the East antenna of Jicamarca were used for comparison with those obtained at Ancón. The signals from the West antenna were not used in this work.

## 4. ANALYSIS OF THE DATA

From our observations of the F-region at Jicamarca a general behavior pattern for the phenomenon is emerging.

Fluctuations usually start after sunset with a thin layer at the bottom edge of the F-region. Later on instabilities develop at different heights usually around the peak of the F layer. The bottom edge fluctuations are persistent and are present most of the time and do not seem to produce amplitude scintillations at Ancón. This general behavior can be observed in Figure 6 where a plot of intensity of scintillations at Ancón is compared with a sample of radar data. Samples are taken every 30 seconds alternatively for each of the Jicamarca antennas, the samples corresponding to the East antenna appear with 100 km height marks.

In Figure 7 a pictorial view of typical nighttime irregularities at Jicamarca is presented and shows the complexity of the phenomenon. In order to compare the Jicamarca and Ancón data a parameterization of them was performed. The analog data collected at Ancón was digitalized, correlated and Fourier analysis was performed. The east channel of Ancón was used to compute the mean value, the mean square and the autocorrelation defined thus,

$$\bar{x} = \frac{1}{N} \sum_{i=1}^{N} x_i \tag{1}$$

$$\overline{x^2} = \frac{1}{N} \sum_{i=1}^{N} (x_i - \bar{x})^2 \tag{2}$$

$$\rho_x(\tau) = \frac{1}{\bar{x}^2} \times \frac{1}{N} \sum_{i=1}^{N} \left[x(t) - \bar{x}\right]\left[x(t_i + \tau) - \bar{x}\right] \tag{3}$$

where N is the number of data points in a sample respectively.

The relative intensity of the scintillations was defined as follows:

$$RI = \frac{\sqrt{\overline{x^2}}}{\overline{x}} \tag{4}$$

The cross correlation between the east and west signals was computed from

$$\rho_{xy}(\tau) = \frac{1}{\sqrt{\overline{x^2}\,\overline{y^2}}} \times \frac{1}{N} \sum_{i=1}^{N} \left[x(t_i) - \overline{x}\right]\left[y(t_i + \tau) - \overline{y}\right] \tag{5}$$

From these computations the E-W velocity of the irregularities can be computed from[2]

$$V = \frac{366}{\tau_m} \tag{6}$$

where

V is the eastward velocity

$\tau_m$ is the time lag at which the maximum of the cross correlation occurs

and

$$\ell = \frac{\tau(\rho_x = \epsilon^{-1})}{V} \tag{7}$$

The Fourier Transform of (3) was computed to obtain the power spectrum of scintillations. Then the spectral width was arbitrarily defined as the frequency at which the power spectrum has decayed near the power level of noise.

To parameterize the Jicamarca data the following assumptions for scintillations were made: ionospheric irregularities cause only random fluctuations of phase on the radio wave coming from ATS-3, then at the bottom of the ionosphere an electromagnetic field distribution with random phases will exist causing random fluctuations of amplitude at the receiving site about 100 km below.

From reference 3, we observe that this model permits one to show that the mean square value of phase fluctuations $\phi^2$ is proportional to the mean square value of

the electron density fluctuations, $\overline{\Delta N^2}$, multiplied by the thickness of the layer. This reference also shows that the relative intensity (RI) of amplitude scintillations is given by

$$RI = K_1 \overline{\phi_0^2} \tag{8}$$

where

$K_1$ is a factor dependent on the wavelength and the size of the irregularities.

In reference 2 we have shown that RI is sensitive to irregularities of sizes in the order of 300 m. It is worth mentioning that the dependence of RI on sizes is wide; that is, the resultant RI on the ground is due to an integration over the whole distribution of sizes. We can say that the process is analogous to an integration produced by a low Q filter.

The backscatter power for the Jicamarca radar is also proportional to $\overline{\Delta N^2}$ and to a term which depends on the scale size of the irregularities. From reference 4, we have that the scale size dependent term is strongly related to irregularities of size $\lambda/2$ only. This means that the backscatter power will be coming fundamentally from irregularities of 3 m size.

The film traces can then be read directly as being proportional to the $\overline{\Delta N^2}$ associated with 3 m irregularities. For the purpose of this report a parameter $I_\phi$ was defined as follows:

$$I_\phi = \sum_{i=1}^{Q} \overline{\Delta N^2}\, \ell_i \qquad \text{arbitrary units} \tag{9}$$

where

$\overline{\Delta N^2}$ is the mean square value of density fluctuations

$\ell_i$ is the elementary thickness of a layer

Q is the number of elementary layers

Then from our previous discussion we have that

$$I_\phi = K_2 \overline{\phi_0^2} \tag{10}$$

where

$K_2$ is a factor dependent on the size of the irregularities

$K_2$ will be zero if no irregularities of size 3 m exist and it will be a constant for a regime in which a given distribution of sizes exist. In general $K_2$ will be time dependent.

Another parameter was defined, the effective thickness of the irregularities,

$$\text{Effective thickness} = \sum_{i=1}^{Q} \ell . \qquad (11)$$

The Jicamarca data film was reduced and then processed to obtain $I_\phi$ from (9) as it is shown in Figure 8.

Both the Jicamarca and Ancón parameters were then plotted together as it is shown in Figure 9, for the observations on September 13.

In Figure 9 we can see that the correlation between $I_\phi$, Jicamarca, and RI, Ancón, is a very complex one. In a general way we can say that correlation is stronger from the beginning of the phenomenon at 8 h 10 m up to about 10 h 10 m.

One of the results that is emerging from these observations is that the thin layer that exists at 300 km bottom edge of the ionosphere, does not correlate with the existence of scintillations. In Figure 10 the lower layer was neglected in the computation of $I_\phi$, it can be seen that this produces a better view of the relationship between $I_\phi$ and RI.

By substituting Equation (10) into Equation (8) we find

$$RI = \left(\frac{K_1}{K_2}\right) I_\phi . \qquad (12)$$

The ratio is expected to be constant under steady state conditions which can not be the case for a period as long as the one shown in Figures 9 and 10. In general the ratio $K_1/K_2$ will be changing with time and will be dependent on irregularity sizes of the order of 200 m to 3 m. Figure 10 shows that the typical sizes for scintillations are changing irregularly during the night, which is a confirmation of the time dependency of $K_1/K_2$.

An extreme situation could happen when $K_2$ is zero, that is when no irregularities of size 3 m exist, in this case the Jicamarca radar will show no echoes. In reference 4 a study of the distribution of scale sizes is made and it is shown that the intensity of ionospheric irregularities, $\overline{\Delta N^2}$, reduces with decreasing size and that the minimum size, that is for which $\overline{\Delta N^2} \approx 0$, is below 100 m. It is then possible that the minimum size is around 3 m and that the fact that Ancón is observing scintillations and Jicamarca is not giving us a strong indication of this.

We can see then that Equation (12) involves a very complex relationship, which is usually the case when the data of two different instruments is analyzed.

But Equation (12) and the previous discussion does not explain why the lower layer, 300 km altitude does not cause scintillations in the majority of the situations. We think that this effect may be related to the fact that this layer is at a height in which the gradient of the electron number density profile is stronger.

The strong gradient that exists at the bottom of the ionosphere should cause a partial reflection of the upgoing energy from the radar. Strong gradients are formed right after sunset when the recombination process in this region reduces the ionization at a fast rate. Measurements of density profiles performed at Jicamarca show that the gradient is actually very high. To estimate the amount of power that is reflected back it was assumed that an infinite gradient exists in this region and then the well known expression for the reflection coefficient was applied. Under this assumption, the reflected power was found to be about 110 db above the maximum incoherent power returned by the ionosphere. That is, under homogeneous conditions in which no irregularities exist, the reflected power of the bottom of the F layer can be up to 11 orders of magnitude higher. Under a finite gradient the reflected power will be lower depending on the gradient itself.

The echo power that we obtain from the lower layer is on the order of 70 db higher than the incoherent scatter power. It could happen that what we observe as the lower layer might be, at first, only a partial reflection and afterwards a gradual development of turbulence. An experiment will be required to confirm the validity of this hypothesis. Such an experiment could use the fact that the layer should be very thin and also aspect sensitive, that is the power should come from a direction normal to the reflecting surface.

The other parameters shown in Figures 9 and 10 also present interesting relationships. It can be seen that the thicker the layer of irregularities are, the higher the intensity of the scintillations become and the wider the power spectrum of scintillations. That is, an increase of the mean square of the fluctuations of phase produce a broadening of the spectrum as in the case of a phase modulated wave in which an increase of the modulation index produce an increase in the bandwidth.

The eastward velocities measured vary without showing any important relationship with the other parameters. The values for the eastward velocity were around 150 m/sec.

The scale sizes seem to decrease with increasing $I_\phi$ and increase with decreasin $I_\phi$ which agrees with the findings of reference 5.

## CONCLUSIONS

The relationships between scintillation observations and backscatter observations are complex and seem to be controlled mainly by the scale size spectrum of irregularities.

Despite the difficulties in correlating the data from Ancón and Jicamarca it has been shown that the method of parameterization produces a cleaner picture of the relationship.

Simultaneous observations of scintillations and backscatter from irregularities produce a more complete picture of the phenomenon and show that perhaps the only way to arrive at a useful model will be to employ a number of different instruments simultaneously.

## REFERENCES


1. G. Tisnado, J. Pomalaza, and R. Woodman, "Statistical Study of Equatorial Scintillations at Ancón," I.G.P. Technical Report 1970.

2. J. Pomalaza, R. Woodman, G. Tisnado, J. Sandoval, and A. Guillen, "A Progress Report on Scintillation Observations at Ancón and Jicamarca Observatories," GSFC X-520-70-398 — October 1970.

3. B. H. Briggs, and I. A. Parkin, "Journal of Atmospheric and Terrestrial Physics," — Vol. 25, No. 6, 1963.

4. C. L. Rufenach, "Wave Number Spectrum."

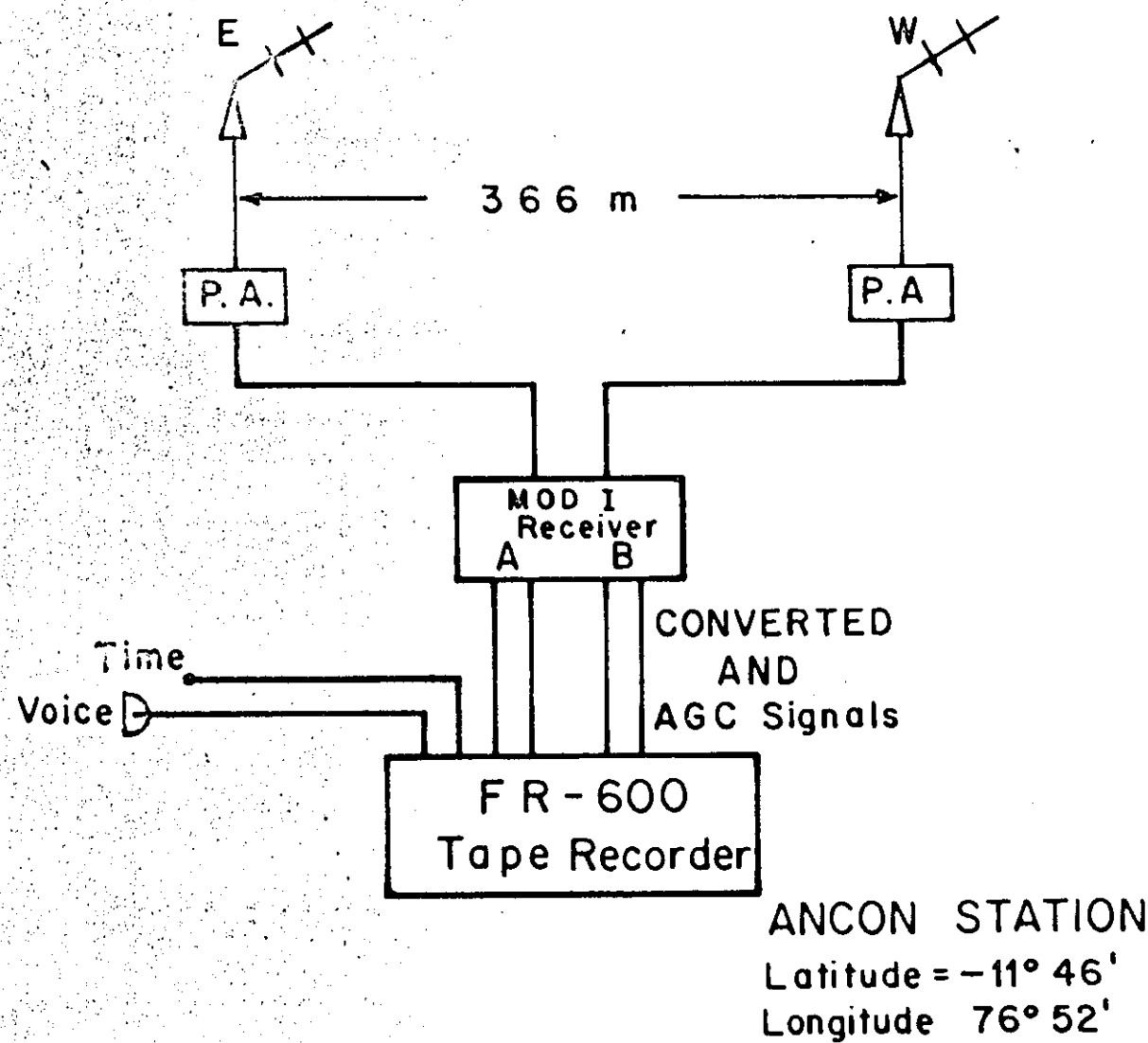


Figure I-1. Block Diagram of 136 MHz System to Record Scintillations at Ancón

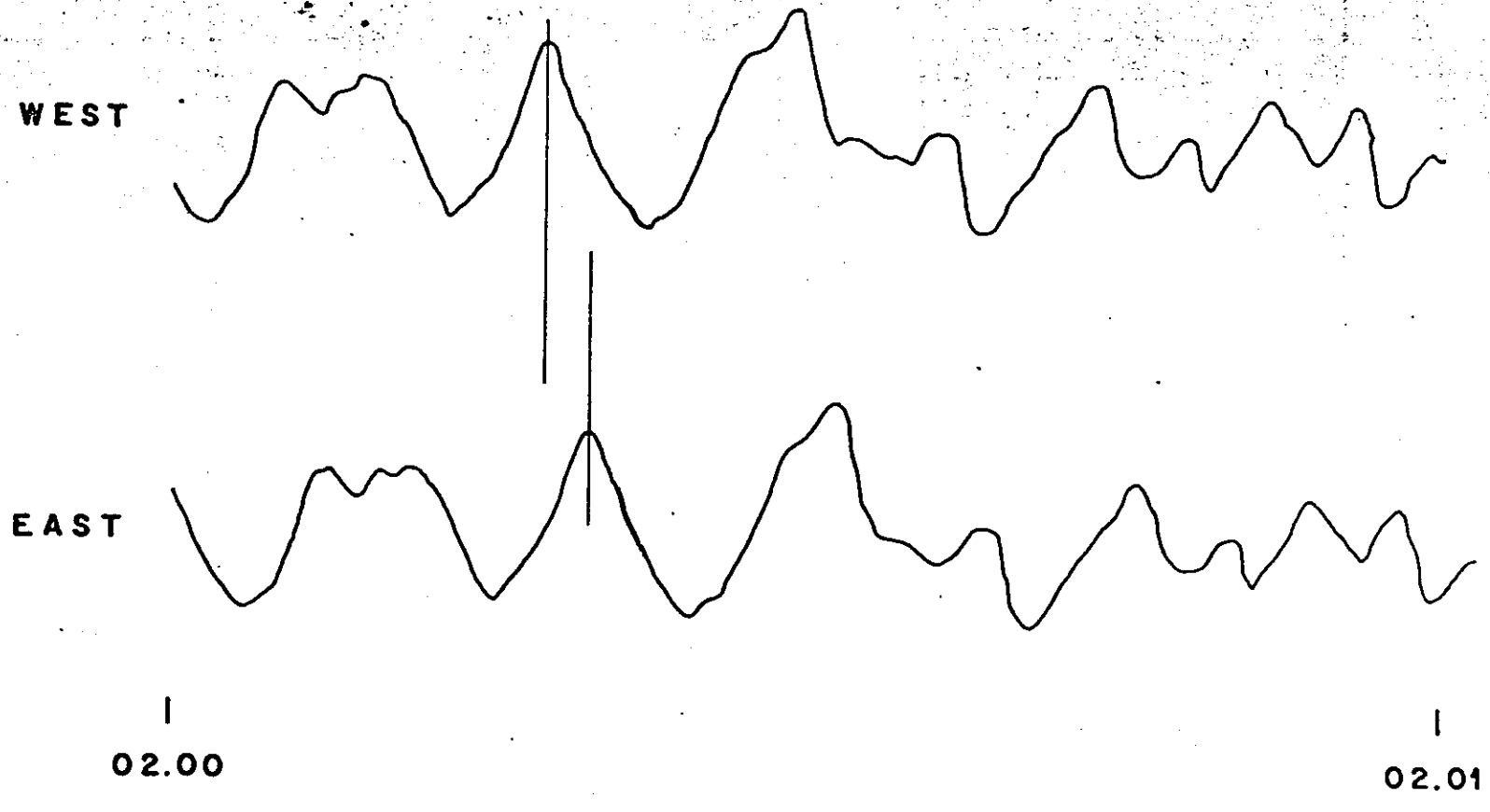


Figure I-2. Typical Amplitude Scintillations for the East and West Channels of the 136 MHz System at Ancón (Time Is Greenwich Mean Time)

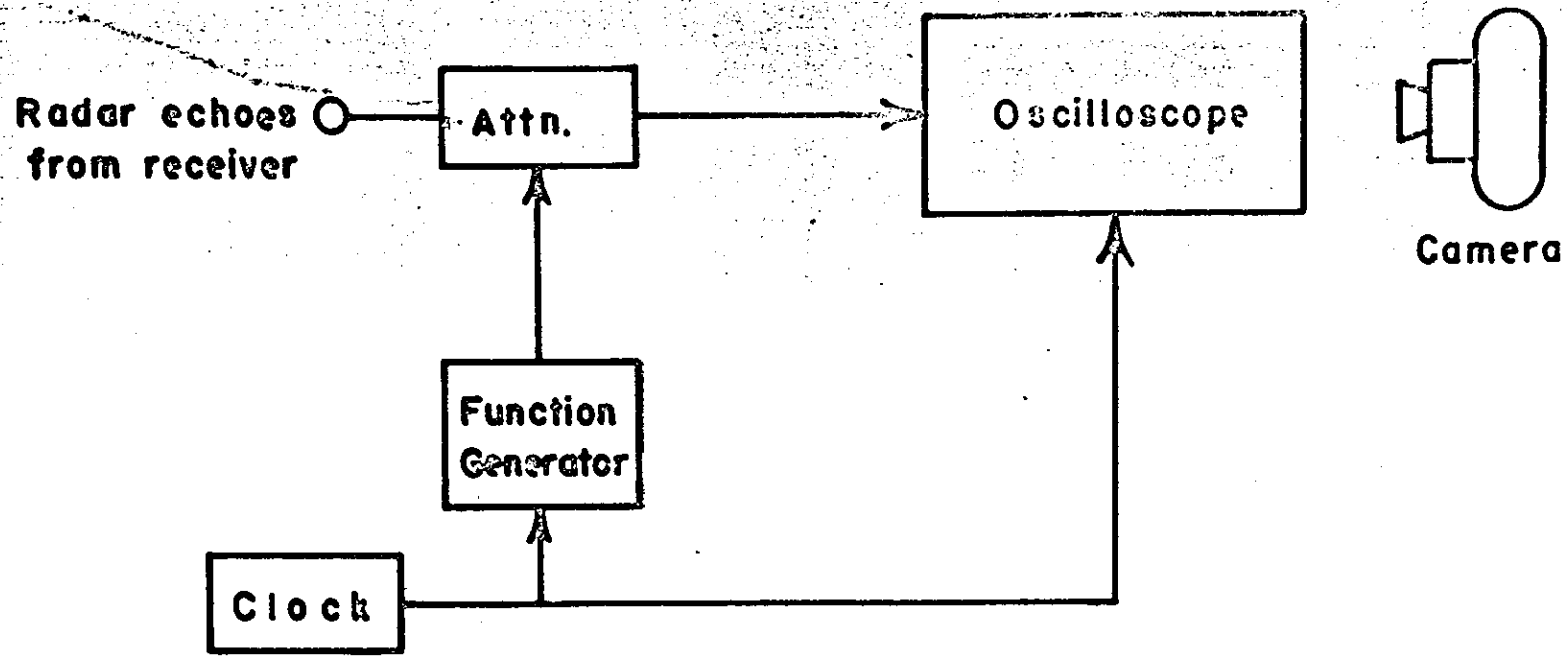


Figure I-3. Block Diagram of the Film Recording System

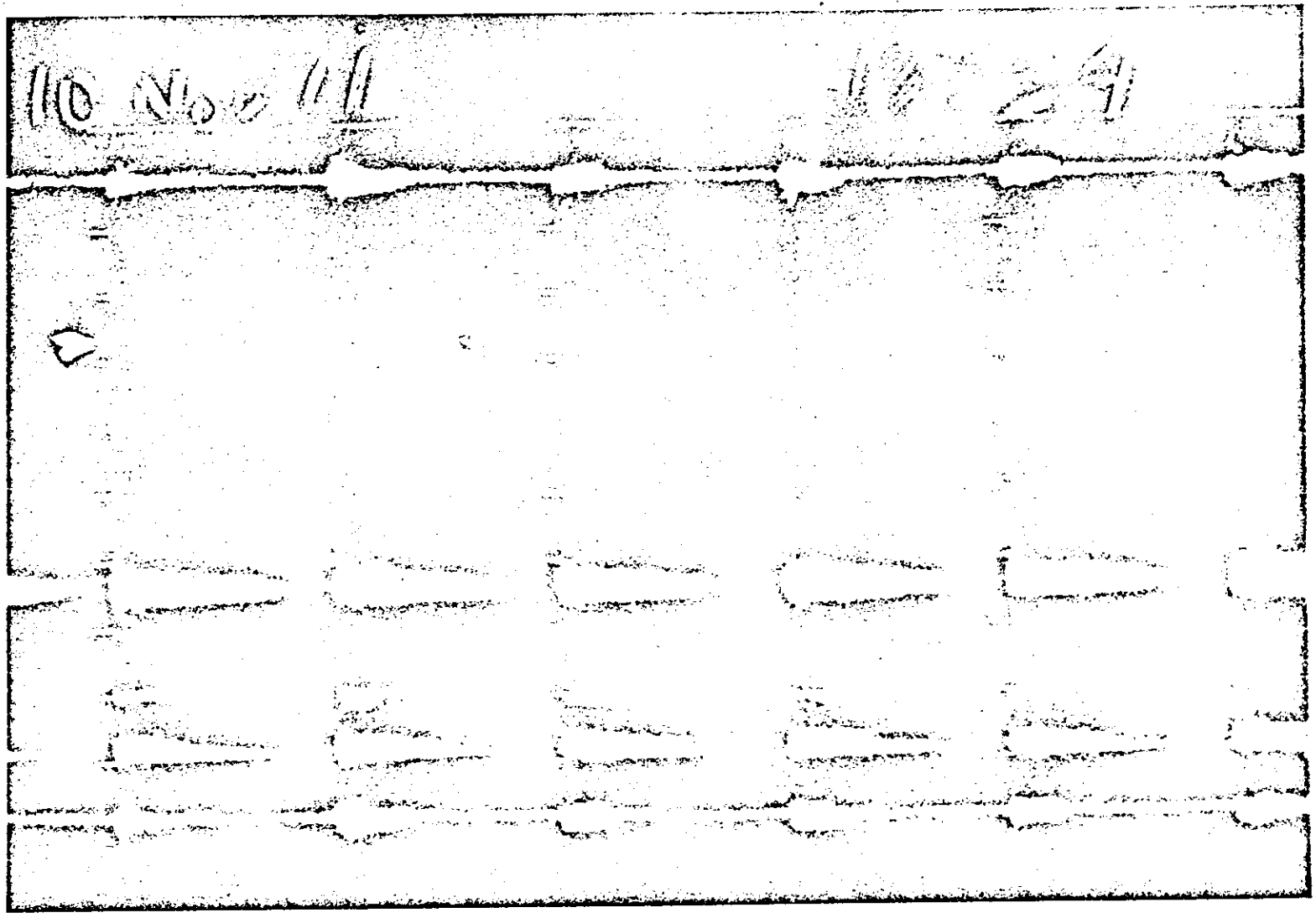

Figure I-4. A Sample of a Picture Obtained with the Film Recording Device

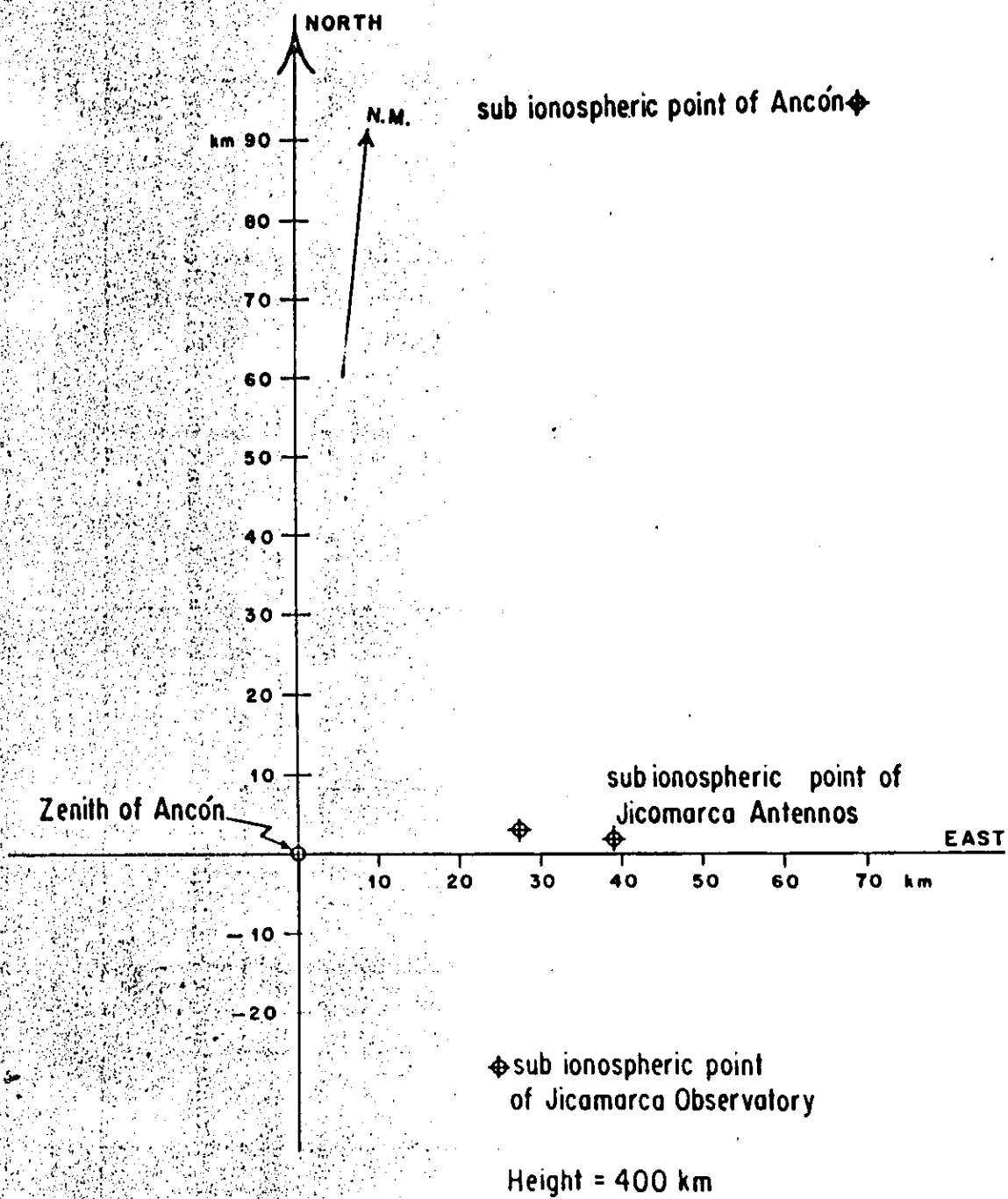


Figure I-5. Geometry During the Observation of September 13

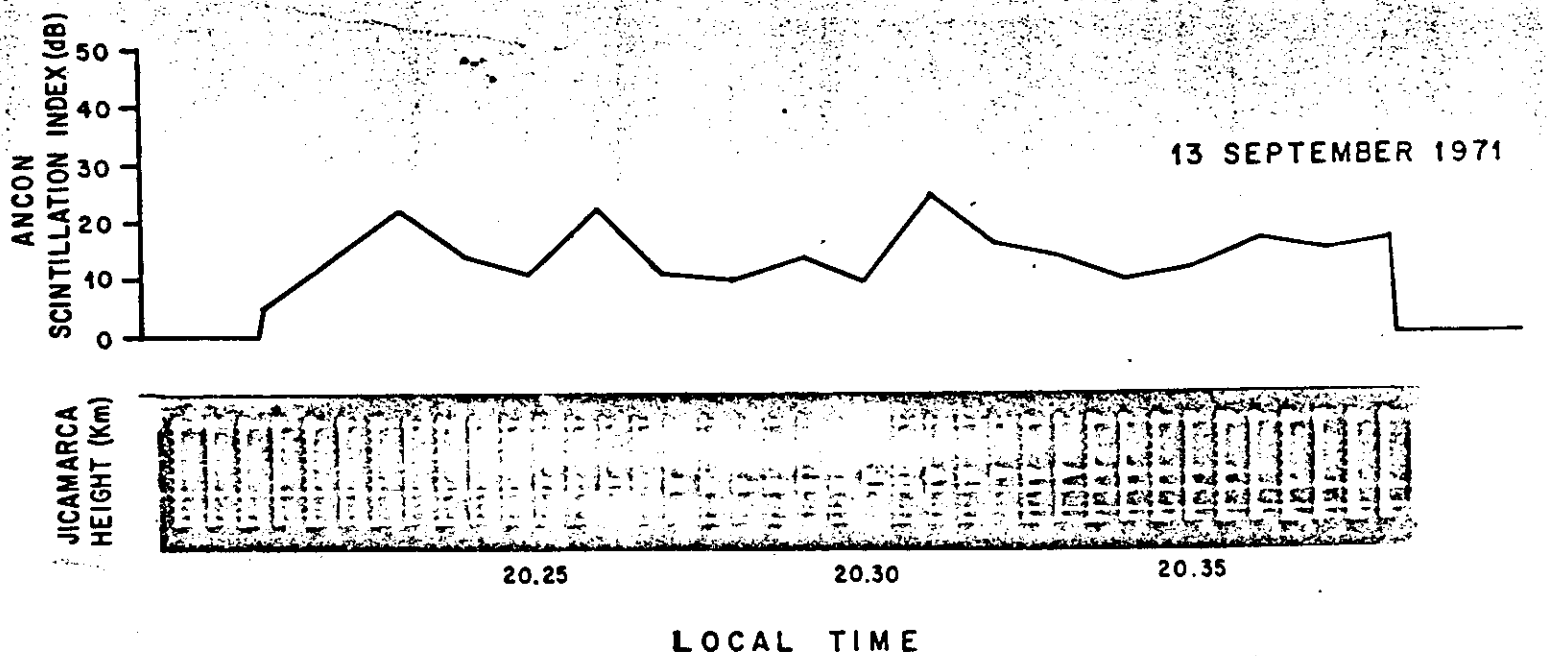


Figure I-6. Comparison of Scintillation Index at Ancón and a Sample of the Film Recorded at Jicamarca

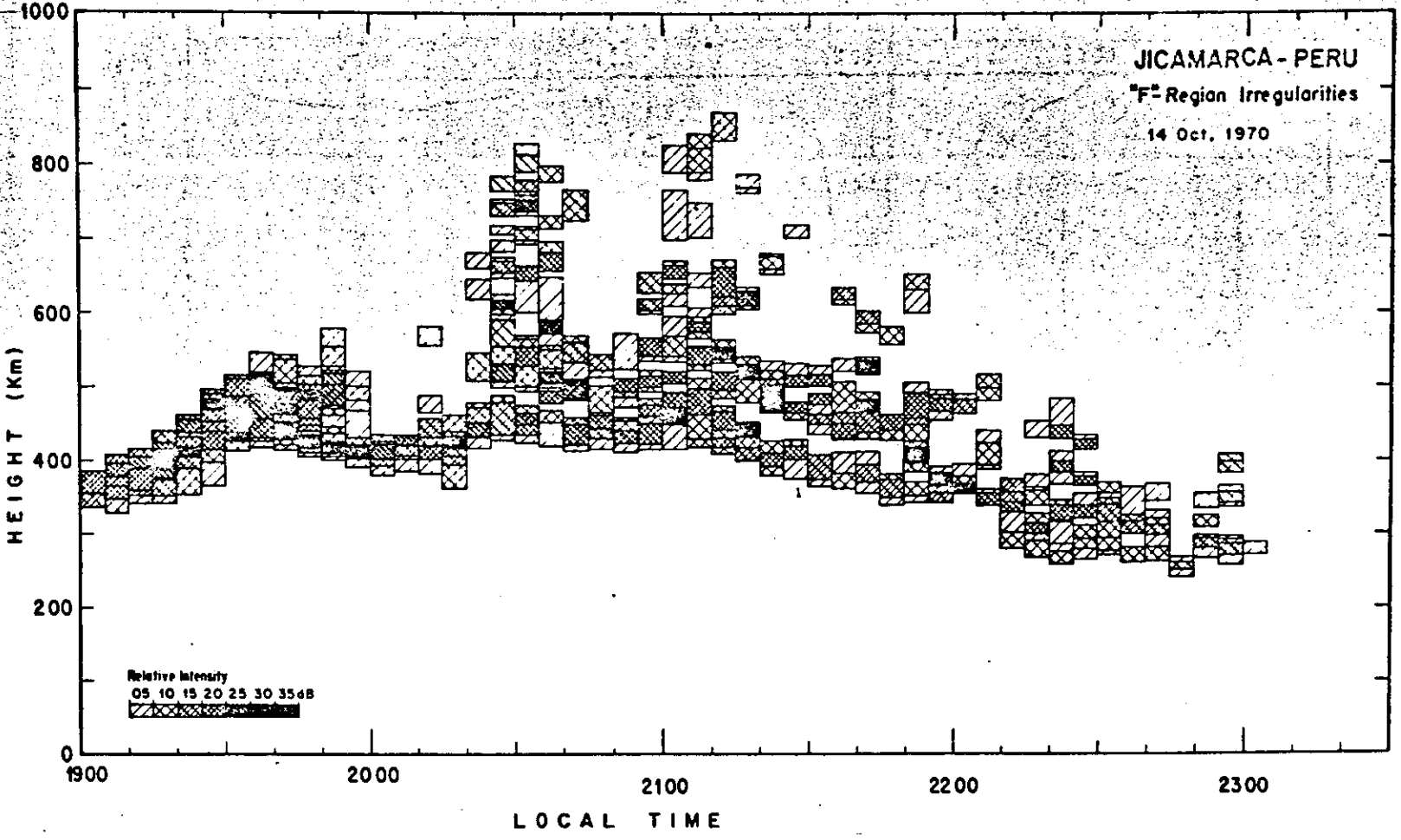


Figure I-7. A Pictorial Representation of the Jicamarca Data

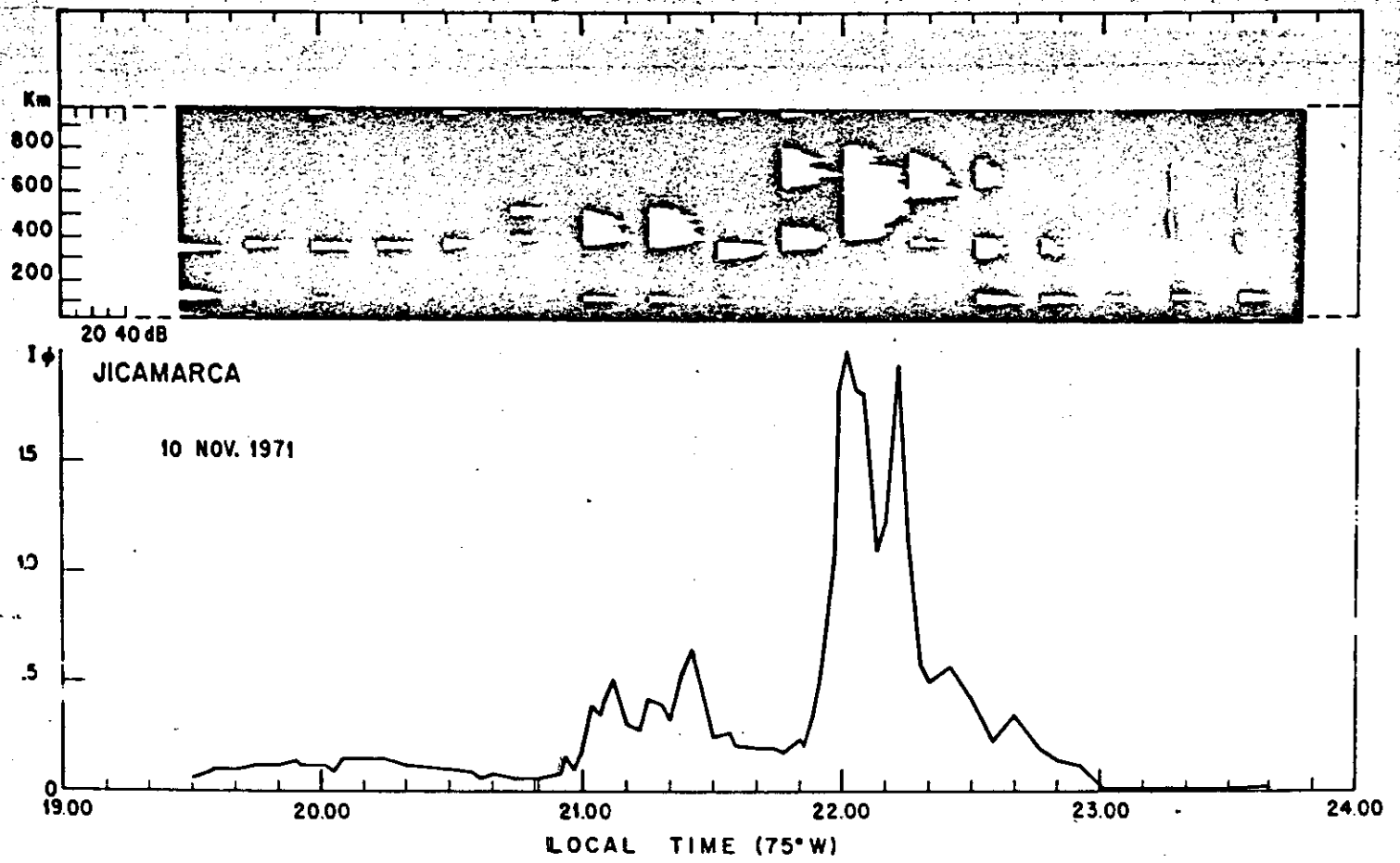


Figure I-8. Am Example of the Computation of $I_\phi$

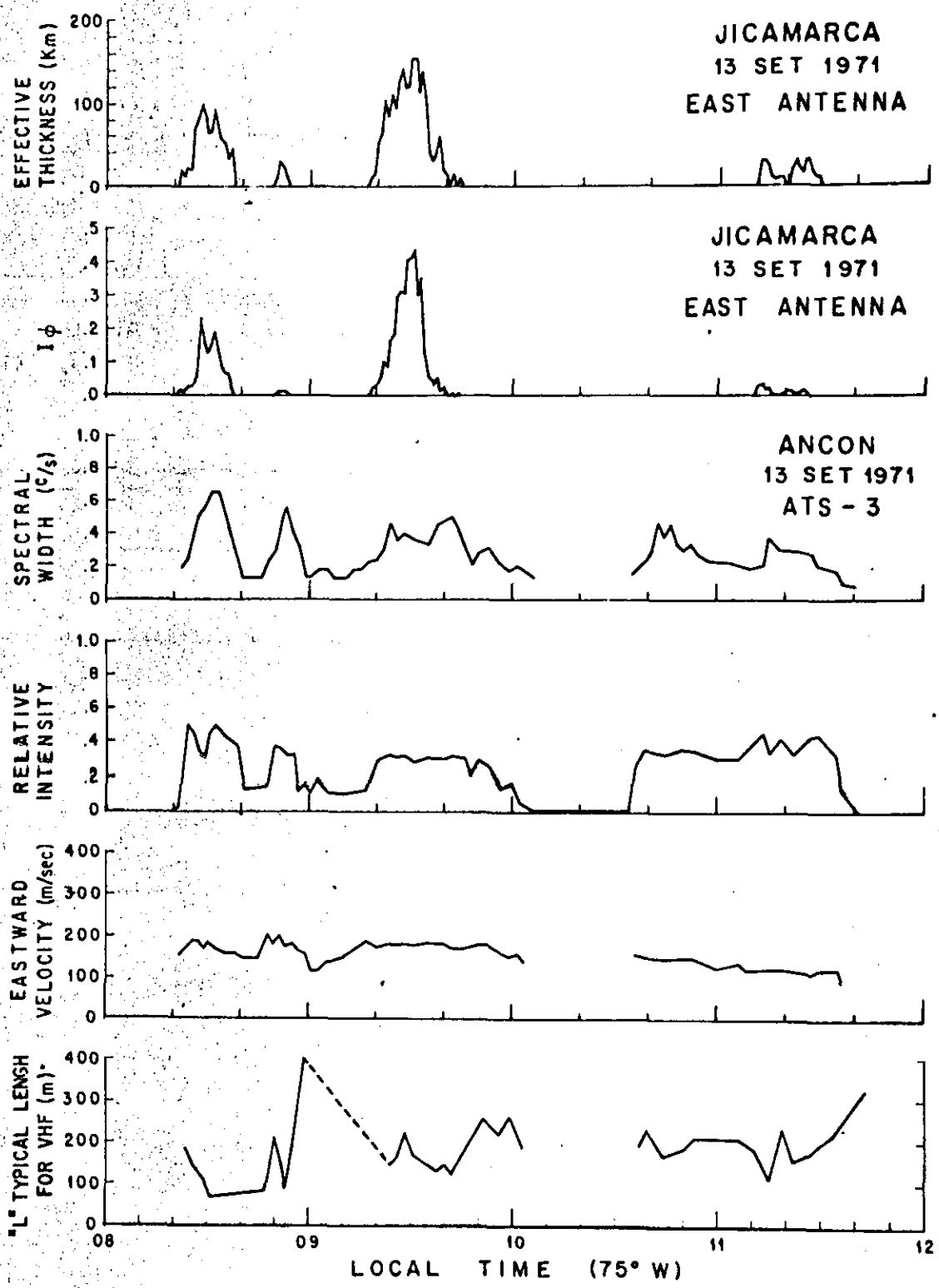


Figure I-10. Ancón and Jicamarca Parameters with the Lower Layer Removed

II

# SIMULTANEOUS OBSERVATIONS OF SCINTILLATIONS AT 136 MHz AND 1550 MHz

## 1. INTRODUCTION

In 1971 a 1550 MHz receiving system was installed at Ancón to make observations of amplitude scintillations using the L-Band transponder of ATS-5.

ATS-5 became defective soon after launching and the L-Band antenna is gyrating with the spacecraft, this causes the received signals to pulsate. A "pulse" is received every time the radiation pattern of the ATS-5 antenna points toward our receiving antenna.

This report includes a brief description of a device designed at Ancón to detect the amplitude scintillations from the pulsating L-Band signals and to perform some of the processing of this data.

## 2. THE L-BAND ENVELOPE DETECTOR

The L-Band receiving system consists of:

- Four foot dish and feed
- Low noise pre-amplifier
- Down converter 1550 MHz to 136 MHz
- L-Band calibrator.

The signals from ATS-5 are down converted to 136 MHz and then feed to a MOD I Telemetry receiver. The AGC output of the MOD I Receiver is then recorded on a strip chart recorder.

Figures 1 and 2 show a typical recording, the upper trace is the decimal coded time and the lower the pulsating signal showing amplitude.

A device that derives a continuous envelope from the pulses was designed and built at Ancón.

Figure 3 shows a block diagram of the envelope detector. The pulsating signal from the MOD I receiver AGC is feed to a pulse shaping device (Schmitt Trigger)

and then a phase lock loop synchronizes an internal stable multivibrator with the input pulses. The pulses from the multivibrator are then used to drive a logic circuit that will hold the maximum value of the pulse until the next pulse has arrived from the receiver. Then a filter is used to obtain a continuous envelope. Figure 3 shows in the lower trace the input to the envelope detector and in the center trace the output.

The equipment works satisfactorily and has permitted us to use the same processing system that was developed for the 136 MHz scintillations [1].

## 3. PROCESSING OF THE L-BAND DATA

Scintillations at L-Band are usually weak in the order of 3 to 5 db's. In some occasions the amplitude fadings can be up to 8 to 10 db's.

Figure 4 shows typical autocorrelation for both 136 MHz and 1550 MHz. It can be seen that no correlation exists between amplitude fluctuations on the two channels. From Figure 4 we can also see that the L-Band correlation times ($\tau$ at which $\rho(\tau) = \epsilon^{-1}$, see reference 1) can be greater, smaller or equal to those at 136 MHz. The case in which the correlation time at L-Band is smaller is less frequent that the others.

Our observations show that the scintillations at VHF have to be strong and well developed before we have L-Band scintillations.

In our previous study we have shown that the spectral width, inversely proportional to the correlation time, increase or decrease depending on the magnitude of $\overline{\Delta\phi^2}$ under strong scintillation conditions. We expect then that in this case correlation times will be varying during the night, the greater $\overline{\Delta\phi^2}$ the smaller the correlation times.

In the case of weak scattering the correlation times multiplied by the drift velocit will give us an estimate of the typical size of the irregularities in the ionosphere[1]

In the typical case observed at Ancón we have strong scintillations in VHF and weak in L-Band. Then we should expect that the correlation times for VHF be smaller than the correlation times for L-Band. But in Part I of this work we have shown how complex is the scintillation phenomenon and that ionospheric conditions are always changing, they are times in which the changes are more frequent and under this dynamic conditions we could have any of the three cases

shown in Figure 4. A more complete analysis of the processed data will be performed in our next report.

REFERENCES

1. Pomalaza et al., "Progress Report on Scintillation Observations at Ancón and Jicamarca Observatories."

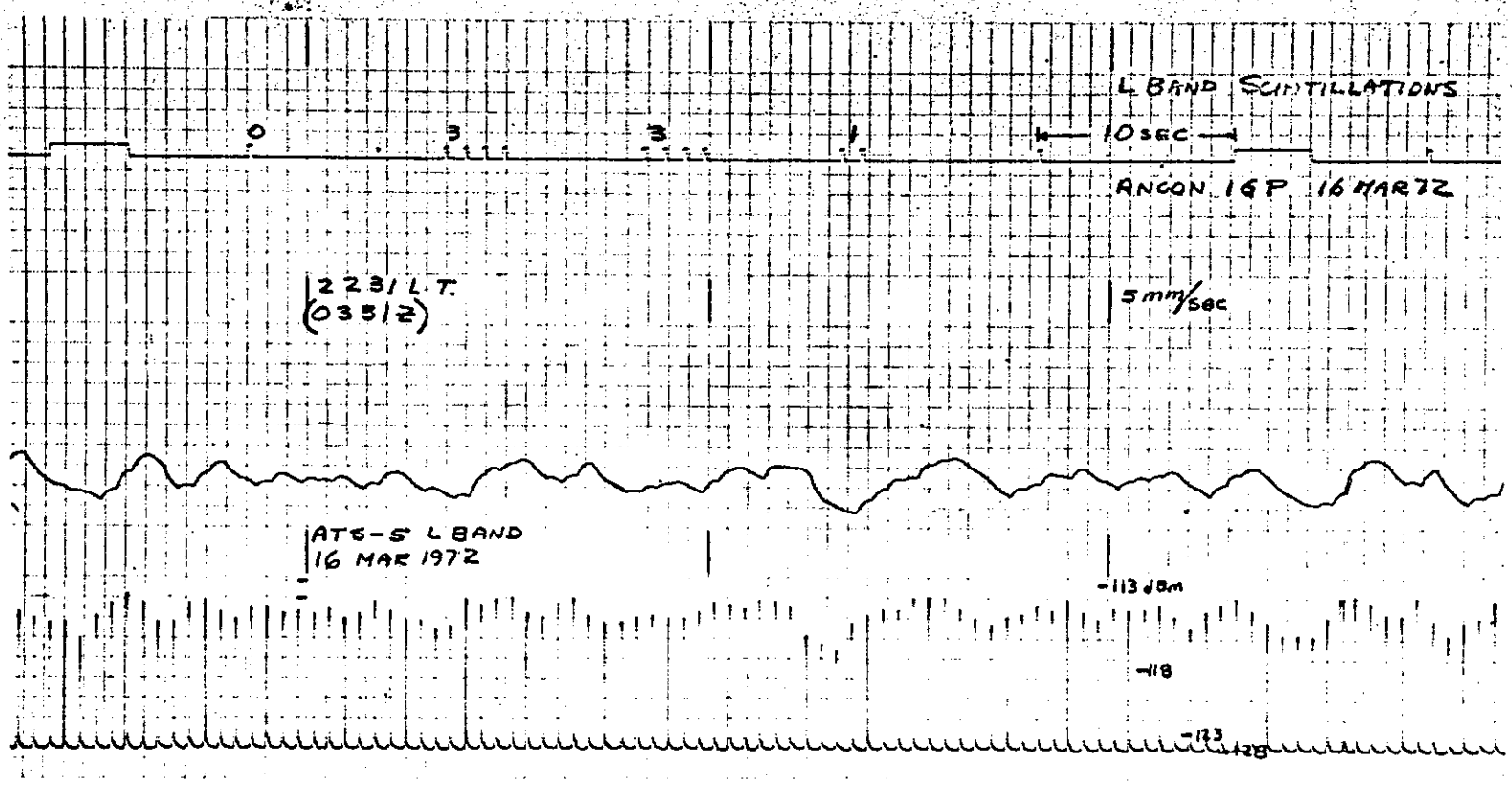


Figure II-1. Sample of a Typical Record for L-Band Scintillations. The Lower Trace Shows the L-Band Pulsating Signal.

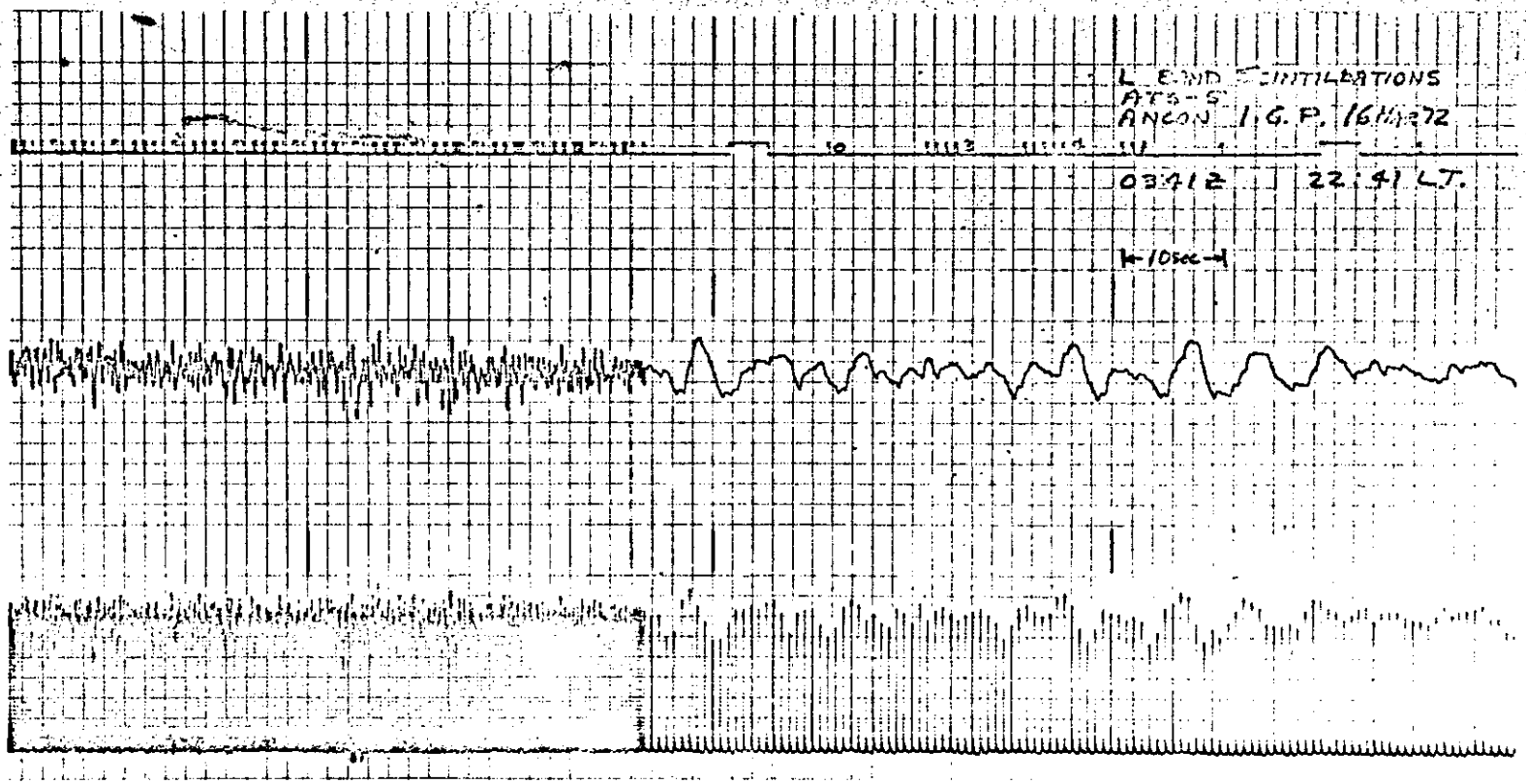


Figure II-2. Performance of the Envelope Detector. The Middle Trace Shows the Output of the Detector.

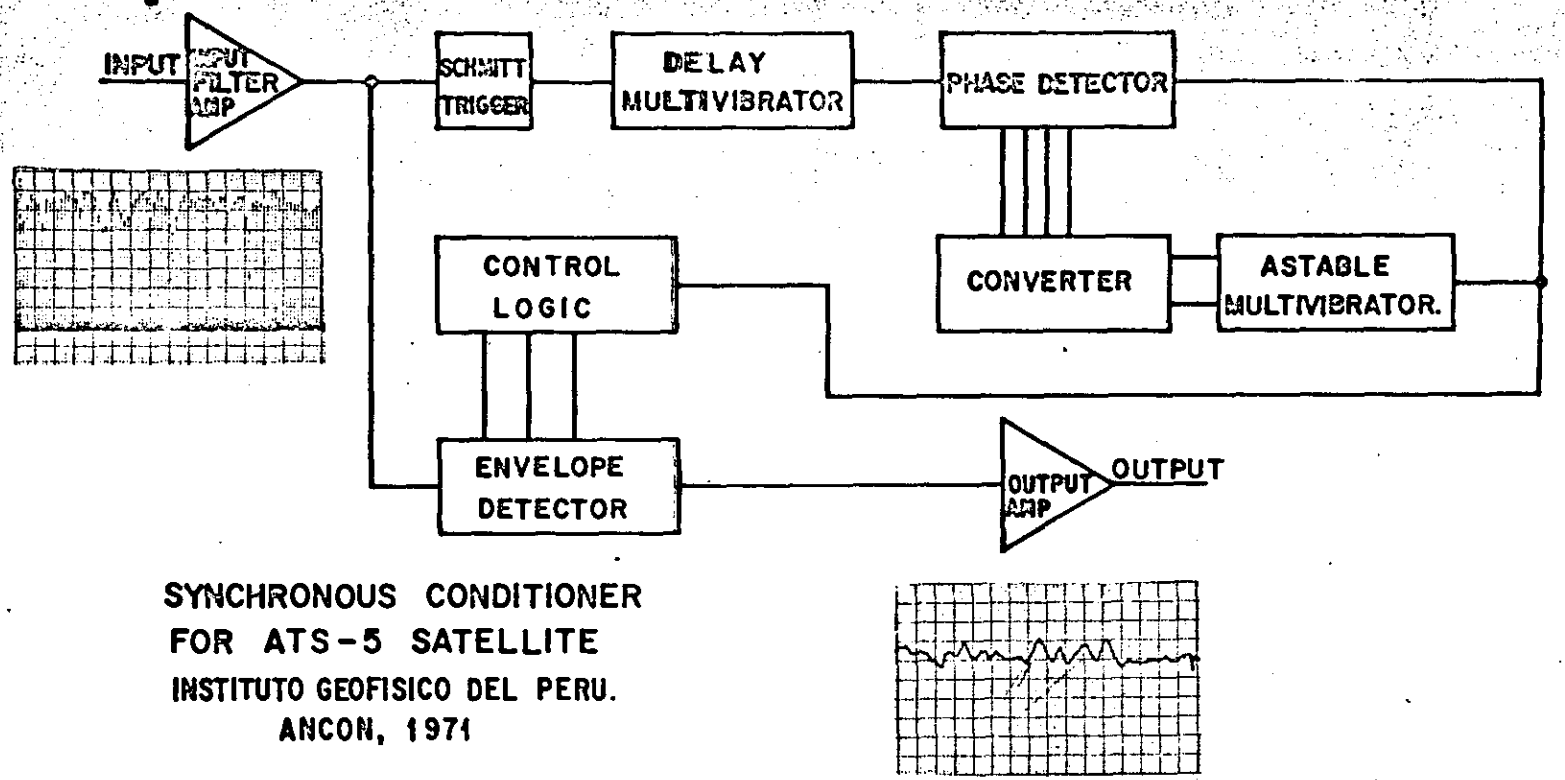


Figure II-3. Block Diagram of the Envelope Detector

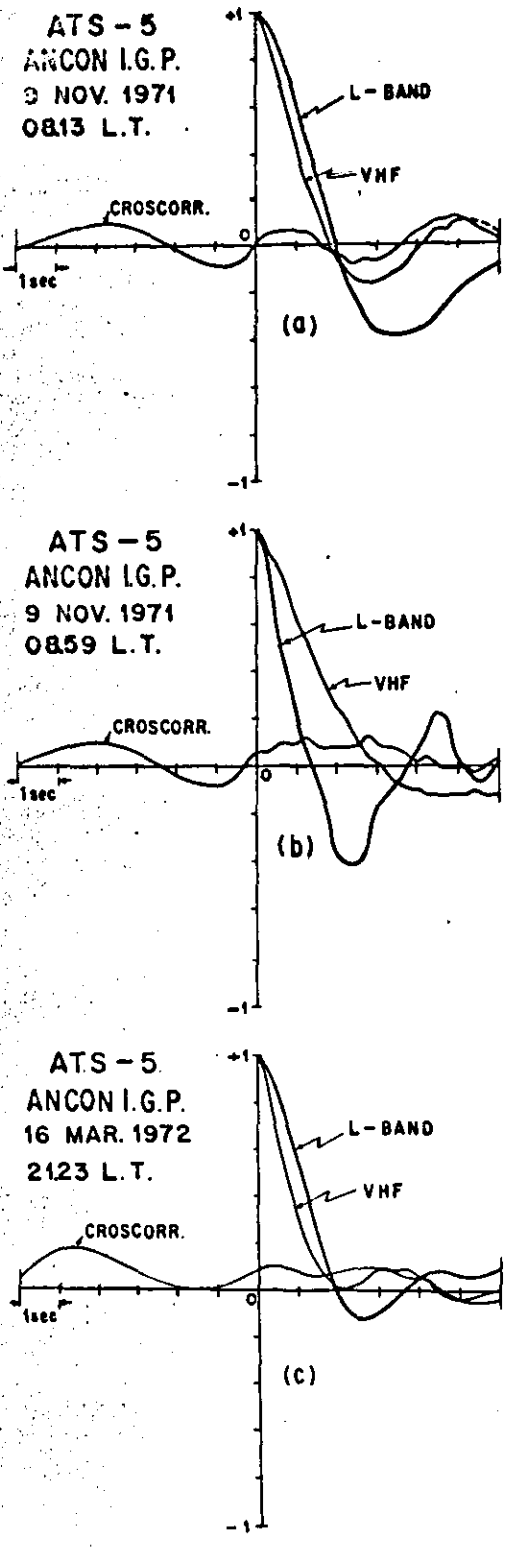


Figure II-4. VHF and L-Band Auto- and Cross-Correlations